

# High-temperature stability study of the oxygen-ion conductor

## $\text{La}_{0.9}\text{Sr}_{0.1}\text{Ga}_{0.8}\text{Mg}_{0.2}\text{O}_{3-x}$

Shanwen Tao,<sup>\*†a,b</sup> Finn Willy Poulsen,<sup>b</sup> Guangyao Meng<sup>a</sup> and Ole Toft Sørensen<sup>b</sup>

<sup>a</sup>Department of Materials Science and Engineering, University of Science and Technology of China, Hefei, Anhui, 230026, China

<sup>b</sup>Materials Research Department, Risø National Laboratory, DK-4000 Roskilde, Denmark

Received 9th May 2000, Accepted 30th May 2000

Published on the Web 13th July 2000

$\text{La}_{0.9}\text{Sr}_{0.1}\text{Ga}_{0.8}\text{Mg}_{0.2}\text{O}_{3-x}$  (LSGM) has been prepared by a complexing sol-gel process and characterised by X-ray diffraction, thermogravimetric-differential thermal analysis (TG-DTA) and conventional weight analysis. The room-temperature structure is orthorhombic, space group *Pnma*, with  $a = 5.5340(14)$ ,  $b = 5.5074(22)$ ,  $c = 7.8003(31)$  Å. After heating at 1000 °C, the lattice parameters of LSGM shift a little, and  $\text{La}_4\text{SrO}_7$  and  $\text{SrLaGaO}_4$  separate from the parent phase, which may further affect other properties. The weight change of LSGM at 750 °C is insignificant and the phase is also stable after heating at 750 °C in a hydrogen atmosphere for a total of 132 h. Defect chemistry modelling supports the view that LSGM is not single phase at 1000 °C.

### 1 Introduction

Because of their high oxygen-ion conductivity,  $\text{LaGaO}_3$ -based perovskites substituted on the A and B sites, such as  $\text{La}_{0.9}\text{Sr}_{0.1}\text{Ga}_{0.8}\text{Mg}_{0.2}\text{O}_{3-x}$  (LSGM), are considered to be promising alternatives to replace yttria-stabilized zirconia (YSZ) currently used in solid oxide fuel cells (SOFCs).<sup>1-7</sup> The mechanical properties<sup>8</sup> and creep behavior<sup>9</sup> of Sr- and Mg-substituted  $\text{LaGaO}_3$  have also been reported. But as an applicable electrolyte for fuel cells, it must fulfil many other requirements, such as thermal and chemical stability, mechanical strength, density, thermal and chemical compatibility with the electrode and interconnector materials, with thermal and chemical stability the primary consideration.<sup>10</sup> It is supposed that Sr- and Mg-substituted  $\text{LaGaO}_3$  is chemically stable over a broad range of oxygen partial pressures because the electrical conductivity remains almost unchanged in the  $P_{\text{O}_2}$  range between  $10^{-23}$  and 1 atm at 850<sup>1</sup> and 800 °C.<sup>5</sup> However, these measurements can only indirectly demonstrate the possible stability of the materials. Thermal analysis and X-ray diffraction (XRD) phase analysis are more direct methods to study the thermal and chemical stability at high temperatures.

Generally,  $\text{La}_{0.9}\text{Sr}_{0.1}\text{Ga}_{0.8}\text{Mg}_{0.2}\text{O}_{3-x}$  might be expected not to react readily with the strong oxidizing agent  $\text{O}_2$  and the strong reducing agent  $\text{H}_2$ . However, several perovskite oxides react with  $\text{CO}_2$  and  $\text{H}_2\text{O}$ .<sup>11,12</sup> It is possible that doped  $\text{LaGaO}_3$  might react with  $\text{CO}_2$  or  $\text{H}_2\text{O}$ , which usually exist under the operating conditions of SOFCs fuelled with  $\text{H}_2$ , CO or  $\text{CH}_4$ . There is also a possibility that secondary phases may separate from the doped  $\text{LaGaO}_3$ , when kept at high temperature for a long time. Furthermore, Djurado and Labeau<sup>13</sup> recently reported that secondary phases formed when sintering the material for longer than 6 h at 1500 °C. The amount of secondary phases formed in a reducing atmosphere was much larger than in an oxidizing atmosphere. This observation causes some doubt as to the long-term stability of LSGM.<sup>13</sup> Recently, Yamaji *et al.*<sup>14</sup> reported the instability of  $\text{La}_{0.9}\text{Sr}_{0.1}\text{Ga}_{0.8}\text{Mg}_{0.2,85}$  at 1000 °C in a humidified reducing atmosphere

because of the sublimation of gallium components such as  $\text{Ga}_2\text{O}$  and formation of  $\text{La}(\text{OH})_3$ . In the present paper, we attempt to determine the thermal and chemical stability of  $\text{La}_{0.9}\text{Sr}_{0.1}\text{Ga}_{0.8}\text{Mg}_{0.2}\text{O}_{3-x}$  at high temperature by thermal and weight analyses as well as room temperature X-ray diffraction phase analyses of heat-treated materials. The data obtained from conventional weight analyses were also analysed by a defect model given by Poulsen and Bonanos.<sup>15,16</sup>

### 2 Experimental

The powder of composition  $\text{La}_{0.9}\text{Sr}_{0.1}\text{Ga}_{0.8}\text{Mg}_{0.2}\text{O}_{3-x}$  was prepared by using the same complexing sol-gel process which has been described elsewhere.<sup>17</sup> Calculated amounts of  $\text{La}_2\text{O}_3$  and  $\text{Ga}_2\text{O}_3$  were first dissolved in dilute  $\text{HNO}_3$  to get a solution. Appropriate amounts of  $\text{Sr}(\text{NO}_3)_2$  and  $\text{Mg}(\text{NO}_3)_2 \cdot 6\text{H}_2\text{O}$  were then added and dissolved in the solution according to the formula  $\text{La}_{0.9}\text{Sr}_{0.1}\text{Ga}_{0.8}\text{Mg}_{0.2}\text{O}_3$ . This solution was carefully dried at 80 °C to remove the excess  $\text{HNO}_3$  and water solvent. An appropriate amount of ethylene glycol was then added to the mixed nitrates and refluxed at 80 °C for 12 h to form a sol. A gel was formed after heating the sol at 120 °C. After pre-firing the gel on an electrical heating plate and calcining above 1200 °C, the Mg- and Sr-doped  $\text{LaGaO}_3$  powder formed.

X-Ray diffraction was carried out with white Cu radiation on a STOE  $\theta$ - $\theta$  reflection diffractometer. The energy dispersive Kevex detector was tuned to the Cu-K $\alpha$  energy (8.04 keV). Lattice parameters were refined with the Visual X<sup>POW</sup> software from STOE. Simultaneous thermogravimetry and differential thermal analyses (TG-DTA) were carried out on the as-prepared doped  $\text{LaGaO}_3$  powders using a thermal analyser (Netzsch STA 429). The samples were heated from room temperature (around 20 °C) to 1200 °C at a heating rate of 2 °C min<sup>-1</sup> and cooled to 100 °C at 5 °C min<sup>-1</sup> in various atmospheres. The conventional weight analyses were carried out *in situ* after heat treatment in a tube furnace under various atmospheres. The purge gas flow rate was 50 ml min<sup>-1</sup>. Humidity was measured by a dewpoint meter (DEWLUXE), from MCM, UK.

<sup>†</sup>Present address: School of Chemistry, University of St Andrews, St Andrews, Fife, Scotland, UK KY16 9ST. E-mail: st21@st-andrews.ac.uk.

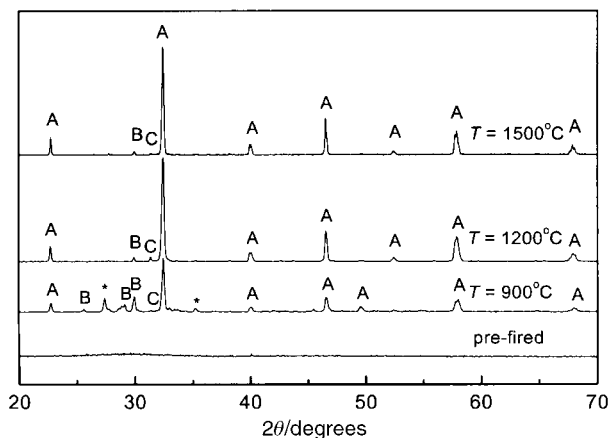


**Fig. 1** X-Ray diffraction patterns of the pre-fired gel and the gel sintered at the temperatures indicated for 5 h. A, B and C indicate diffraction peaks due to LaGaO<sub>3</sub>, La<sub>4</sub>SrO<sub>7</sub> and SrLaGaO<sub>4</sub>, respectively. \* denotes unidentified peaks.

### 3 Results and discussion

#### 3.1 Preparation of doped LaGaO<sub>3</sub>

The X-ray diffraction patterns of Sr- and Mg-doped LaGaO<sub>3</sub> prepared by the sol-gel process and calcined at various temperatures are shown in Fig. 1. The pre-fired powder is mainly composed of amorphous phases. These phases could be single or complex oxides decomposed from the organic precursors in the xerogel. When calcining the pre-fired powder at 900 °C for 5 h, the LaGaO<sub>3</sub> phase (orthorhombic, JCPDS card No. 24-1102) was mainly formed. Besides LaGaO<sub>3</sub>, peaks of La<sub>4</sub>SrO<sub>7</sub> were also observed as well as some unknown ones. The peak around  $d = 2.98$  Å belonging to SrLaGaO<sub>4</sub> is quite weak. Increasing the calcining temperature to 1200 °C, some peaks belonging to La<sub>4</sub>SrO<sub>7</sub> disappear except the one around  $d = 2.85$  Å. The relative intensity of the peak for SrLaGaO<sub>4</sub> increases a little when calcining the sample at 1200 °C. The weak peaks of La<sub>4</sub>SrO<sub>7</sub> and SrLaGaO<sub>4</sub> still exist in the powder although it is sintered at 1500 °C for 5 h. Similar to LaGaO<sub>3</sub>, the phases La<sub>4</sub>SrO<sub>7</sub> and SrLaGaO<sub>4</sub> are also thermodynamically stable between 900–1500 °C. In previous reports, these two impurity phases were also found in Sr- and Mg-doped LaGaO<sub>3</sub>, when prepared by a solid state reaction.<sup>2,7</sup> Djurado and Labeau<sup>13</sup> have prepared Sr- and Mg-doped lanthanum gallate by solid state reactions and by an ultrasonic spray pyrolysis method. La<sub>2</sub>O<sub>3</sub>, MgO, LaSrGa<sub>3</sub>O<sub>7</sub>, Sr<sub>3</sub>Ga<sub>2</sub>O<sub>6</sub>, La<sub>4</sub>Ga<sub>2</sub>O<sub>9</sub>, La<sub>3</sub>Ga<sub>5</sub>O<sub>12</sub>, MgGa<sub>2</sub>O<sub>4</sub>, La<sub>2</sub>SrO<sub>x</sub> and LaSrGaO<sub>4</sub> were found as second phase impurities in the synthesized samples. The impurity phases are strongly related to the preparation methods; various impurities appear when different methods are applied. The La<sub>0.9</sub>Sr<sub>0.1</sub>Ga<sub>0.8</sub>Mg<sub>0.2</sub>O<sub>3</sub> prepared by the method described in this paper contains only trace amounts of La<sub>4</sub>SrO<sub>7</sub> and SrLaGaO<sub>4</sub> impurities.

#### 3.2 TG-DTA analyses

TG-DTA was used to analyse the thermal and chemical stability of the La<sub>0.9</sub>Sr<sub>0.1</sub>Ga<sub>0.8</sub>Mg<sub>0.2</sub>O<sub>3</sub> powder obtained at 1500 °C. Fig. 2 shows the TG-DTA results in wet air. The wet air was obtained by passing dry air through water at 10 °C. During the equilibration process, the weight of the powder increased by 0.04 wt%. The colour of the powder did not change after the TG-DTA measurement. The TG-DTA results for the La<sub>0.9</sub>Sr<sub>0.1</sub>Ga<sub>0.8</sub>Mg<sub>0.2</sub>O<sub>3</sub> powder in an atmosphere containing 9% hydrogen and 91% nitrogen are shown in Fig. 3. In both figures an uncompensated baseline drift is observed, while only in Fig. 3 is a permanent weight loss observed. The weight change above 1000 °C can be attributed mainly to the loss of lattice oxygen and the sublimation of

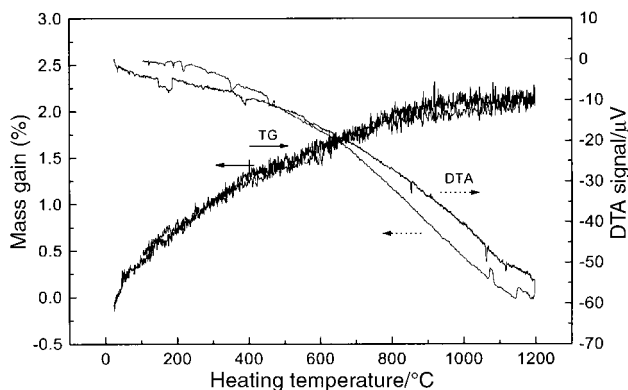


**Fig. 2** TG-DTA traces of La<sub>0.9</sub>Sr<sub>0.1</sub>Ga<sub>0.8</sub>Mg<sub>0.2</sub>O<sub>3-x</sub> in wet air.

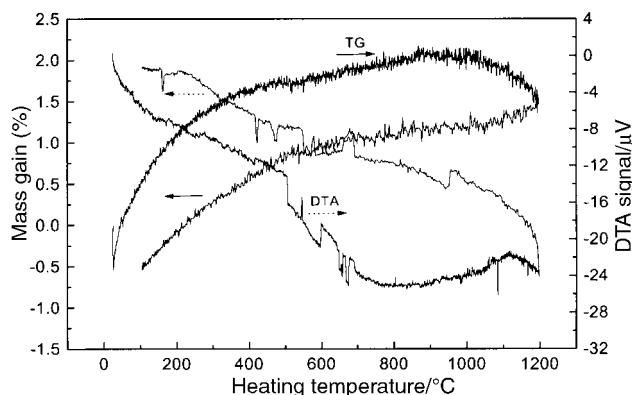
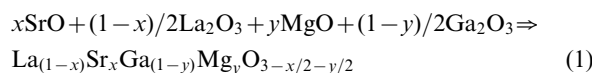


**Fig. 3** TG-DTA traces of La<sub>0.9</sub>Sr<sub>0.1</sub>Ga<sub>0.8</sub>Mg<sub>0.2</sub>O<sub>3-x</sub> in 9% H<sub>2</sub>-91% N<sub>2</sub>.

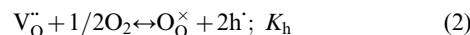
gallium components, such as Ga<sub>2</sub>O, at high temperature in a reducing atmosphere.<sup>14</sup> After the TG-DTA measurement in 9% H<sub>2</sub>-91% N<sub>2</sub>, the colour of the powder had changed from brown to grey.

In the Sr- and Mg-doped LaGaO<sub>3</sub>, oxygen vacancies are introduced by substitution of Sr<sup>2+</sup> for La<sup>3+</sup> and Mg<sup>2+</sup> for Ga<sup>3+</sup> ions, according to the following:



It is clear from this formula that the doped compound should have a plateau in oxygen content corresponding to 2.85 oxide ions per formula unit in a large  $P_{\text{O}_2}$  range, if LSGM is assumed to be a pure or close to pure oxygen ion conductor. This corresponds to  $[V_{\text{O}}^{\bullet}] \approx 0.15$ . In the above, the formation of a small amount of second phases has been neglected.

The oxygen ion vacancies created are in equilibrium with atmospheric oxygen according to the following equilibrium equation, using  $K_h$  as defined in eqn. (7) and eqn. (10) below:



In a hydrogen atmosphere, where the oxygen partial pressure is quite low, eqn. (2) will be displaced towards the left-hand side. The lattice oxygen in the La<sub>0.9</sub>Sr<sub>0.1</sub>Ga<sub>0.8</sub>Mg<sub>0.2</sub>O<sub>3</sub> will therefore combine with electron holes and oxygen will be released, resulting in a weight loss. In this case, the concentration of electron holes decreases. When the oxygen partial pressure is high, the main defects in La<sub>0.9</sub>Sr<sub>0.1</sub>Ga<sub>0.8</sub>Mg<sub>0.2</sub>O<sub>3</sub> are oxygen-ion vacancies and electron holes. The decrease of electron hole concentration in a reducing atmosphere might bleach the La<sub>0.9</sub>Sr<sub>0.1</sub>Ga<sub>0.8</sub>Mg<sub>0.2</sub>O<sub>3</sub> powder. On heating the grey La<sub>0.9</sub>Sr<sub>0.1</sub>Ga<sub>0.8</sub>Mg<sub>0.2</sub>O<sub>3</sub> powder at 750 °C for 12 h in air, it regained its initial brown colour. The endothermic effect above 500 °C on the DTA curve of Fig. 3 observed under a reducing atmosphere might be due to the release of lattice oxygen and sublimation of

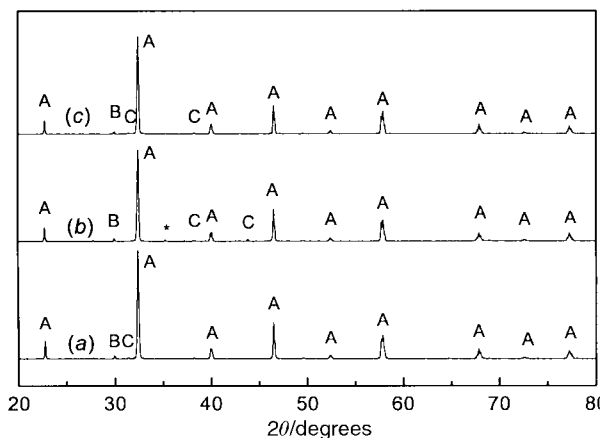


**Fig. 4** X-Ray diffraction patterns of (a)  $\text{La}_{0.9}\text{Sr}_{0.1}\text{Ga}_{0.8}\text{Mg}_{0.2}\text{O}_{3-x}$  obtained at  $1500^\circ\text{C}$  after 5 h, (b)  $\text{La}_{0.9}\text{Sr}_{0.1}\text{Ga}_{0.8}\text{Mg}_{0.2}\text{O}_{3-x}$  after TG-DTA analysis in wet air up to  $1200^\circ\text{C}$  and (c)  $\text{La}_{0.9}\text{Sr}_{0.1}\text{Ga}_{0.8}\text{Mg}_{0.2}\text{O}_{3-x}$  after TG-DTA analysis in 9 mol%  $\text{H}_2$ -91 mol%  $\text{N}_2$  up to  $1200^\circ\text{C}$ . A, B, C and \* indicate  $\text{LaGaO}_3$ ,  $\text{La}_4\text{SrO}_7$ ,  $\text{SrLaGaO}_4$  and unidentified phases, respectively.

gallium components from the  $\text{La}_{0.9}\text{Sr}_{0.1}\text{Ga}_{0.8}\text{Mg}_{0.2}\text{O}_3$  accompanied by weight loss. On the other hand, the weight change and thermal effects of the material in wet air (Fig. 2) were not significant.

Fig. 4 shows the X-ray diffraction patterns of the  $\text{La}_{0.9}\text{Sr}_{0.1}\text{Ga}_{0.8}\text{Mg}_{0.2}\text{O}_3$  powders after the TG-DTA analyses in wet air and 9%  $\text{H}_2$ -91%  $\text{N}_2$ . For comparison, the pattern of  $\text{La}_{0.9}\text{Sr}_{0.1}\text{Ga}_{0.8}\text{Mg}_{0.2}\text{O}_3$  powder before TG-DTA analyses is also shown. After the TG-DTA tests up to  $1200^\circ\text{C}$ , new weak peaks of  $\text{SrLaGaO}_4$  were found in the sample tested in both wet air and 9% hydrogen. For the sample which underwent TG-DTA analysis in wet air, an unknown peak was also observed. These observations indicate that  $\text{SrLaGaO}_4$  or another impurity phase may separate from the  $\text{La}_{0.9}\text{Sr}_{0.1}\text{Ga}_{0.8}\text{Mg}_{0.2}\text{O}_3$  phase at high temperature. In order to study the long-term stability of  $\text{La}_{0.9}\text{Sr}_{0.1}\text{Ga}_{0.8}\text{Mg}_{0.2}\text{O}_3$  at high temperature in different atmo-

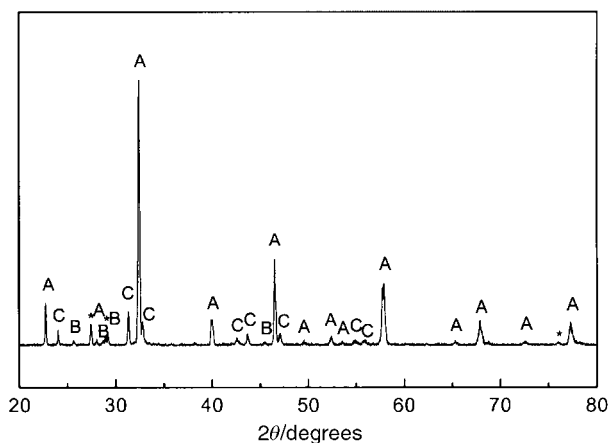


**Fig. 5** X-Ray diffraction patterns of the samples after the weight analyses at  $1000^\circ\text{C}$ . A, B, C and \* indicate diffraction peaks due to  $\text{LaGaO}_3$ ,  $\text{La}_4\text{SrO}_7$ ,  $\text{SrLaGaO}_4$  and unidentified phases, respectively.

**Table 1** Weight and colour change of  $\text{La}_{0.9}\text{Sr}_{0.1}\text{Ga}_{0.8}\text{Mg}_{0.2}\text{O}_{3-x}$  in different atmospheres at  $1000^\circ\text{C}$  overnight (12–14 h)

Atmosphere	$\text{O}_2$	Air	$\text{N}_2$	9% $\text{H}_2$ -91% $\text{N}_2$	$\text{H}_2$
Weight in dry gas/g	0.6862	0.6836	0.6821	0.6761	0.6546
$(W_g - W_{\text{air}})/W_{\text{air}} \times 100$ (%) <sup>a</sup>	+0.38	0	-0.21	-1.10	-4.24
Colour	brown	brown	brown	grey	grey
Weight in wet gas (0.6 vol% $\text{H}_2\text{O}$ )/g	0.6552	0.6550	0.6533	0.6536	0.6463
$(W_g - W_{\text{air}})/W_{\text{air}} \times 100$ (%) <sup>a</sup>	+0.03	0	-0.26	-0.21	-1.33
Colour	brown	brown	brown	grey	grey

<sup>a</sup> $W_g$  is the weight of sample in different atmospheres.  $W_{\text{air}}$  is the weight of sample in dry and wet air respectively.

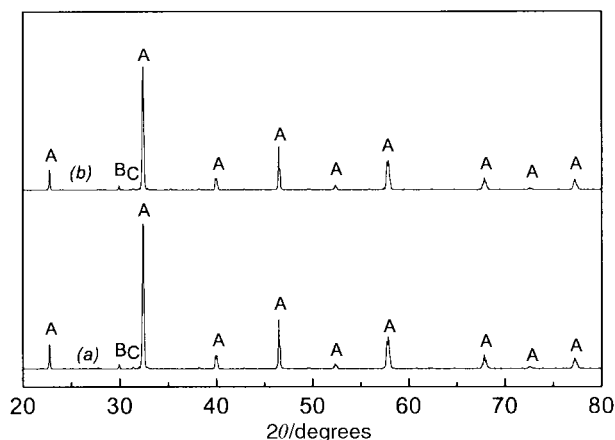


**Fig. 6** X-Ray diffraction patterns of (a)  $\text{La}_{0.9}\text{Sr}_{0.1}\text{Ga}_{0.8}\text{Mg}_{0.2}\text{O}_{3-x}$  obtained at  $1500^\circ\text{C}$ , 5 h, and (b)  $\text{La}_{0.9}\text{Sr}_{0.1}\text{Ga}_{0.8}\text{Mg}_{0.2}\text{O}_{3-x}$  after the weight analyses at  $750^\circ\text{C}$ . A, B, C indicate diffraction peaks of  $\text{LaGaO}_3$ ,  $\text{La}_4\text{SrO}_7$  and  $\text{SrLaGaO}_4$ , respectively.

spheres, conventional weight analysis was introduced for further investigation.

### 3.3 Conventional weight analyses

An alumina boat was heated at high temperature to remove the absorbed water and other impurities before weighing. Then  $\text{La}_{0.9}\text{Sr}_{0.1}\text{Ga}_{0.8}\text{Mg}_{0.2}\text{O}_3$  powder was put into the boat, heated at  $1000^\circ\text{C}$  overnight (12–14 h). After this, the furnace temperature was decreased to about  $50^\circ\text{C}$ , the powder was removed and weighed immediately. The same powder was then heated in pure oxygen, nitrogen, hydrogen or 9%  $\text{H}_2$ -91%  $\text{N}_2$ , using the same process. The results of conventional weight analyses are shown in Table 1 and in Fig. 7. The weight changes in dry gases monotonically depend on the oxygen partial pressure. The weight increased in oxygen and decreased in nitrogen and hydrogen. These changes follow the trend predicted by eqn. (2), which is displaced under a different oxygen partial pressure. When heating the powder in wet

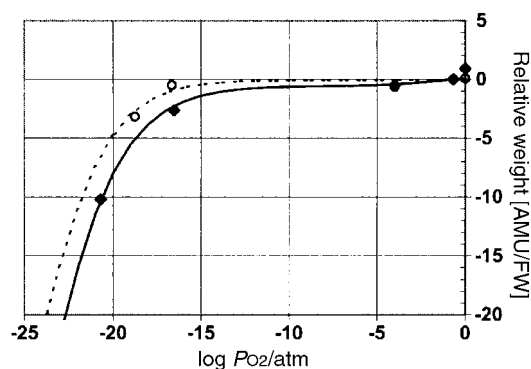


**Fig. 7** Experimental and calculated relative weight at  $1000^\circ\text{C}$  for two series of measurements at  $P_{\text{H}_2\text{O}} = 8.4 \times 10^{-4}$  (dry, open symbols) and  $6 \times 10^{-3}$  atm (wet, filled symbols), respectively. The calculated weight curves were generated from  $K_{\text{H}} = 1940 \text{ atm}^{-1}$ ,  $K_{\text{h}} = 11.0 \text{ atm}^{-1/2}$ , and  $K_{\text{e}} = 4.5 \text{ atm}^{1/2}$ .

atmospheres, in general, the weight change is less significant than that in dry atmospheres; the mass loss is 4.24% in dry hydrogen but only 1.33% in wet hydrogen. The oxygen partial pressure is higher in wet hydrogen according to the equilibrium equation:



In this case, the oxygen partial pressure in wet oxygen is also a little lower than in dry oxygen. This significant mass loss cannot be explained by a displacement of eqn. (2) only. It can for the most part be attributed to the sublimation of gallium components in a reducing atmosphere. The weight of  $\text{La}_{0.9}\text{Sr}_{0.1}\text{Ga}_{0.8}\text{Mg}_{0.2}\text{O}_3$  in dry oxygen increases by 0.38%, but by only 0.03% in wet oxygen.

After all these conventional weight analyses at 1000 °C listed in Table 1, the powder was tested by X-ray diffraction at room temperature (Fig. 5). It is obvious that the intensity of the  $\text{La}_4\text{SrO}_7$  and  $\text{SrLaGaO}_4$  peaks increase significantly. Three unidentified peaks also appear. The segregation of the impurities  $\text{La}_4\text{SrO}_7$ ,  $\text{SrLaGaO}_4$  and the unidentified phases from  $\text{La}_{0.9}\text{Sr}_{0.1}\text{Ga}_{0.8}\text{Mg}_{0.2}\text{O}_3$  indicate that the material is unstable at 1000 °C. The instability of  $\text{La}_{0.9}\text{Sr}_{0.1}\text{Ga}_{0.8}\text{Mg}_{0.2}\text{O}_3$  at 1500 °C has been demonstrated by Djurado and Labeau.<sup>13</sup> The segregation of degradation products may destroy the structure of  $\text{La}_{0.9}\text{Sr}_{0.1}\text{Ga}_{0.8}\text{Mg}_{0.2}\text{O}_3$ , decrease the concentration of oxygen vacancies and further decrease the oxygen-ion conductivity.<sup>18</sup> In practice, the electrolyte has to be sintered at high temperature (usually above 1200 °C) when fabricating fuel cells. Therefore, the sintering of  $\text{La}_{0.9}\text{Sr}_{0.1}\text{Ga}_{0.8}\text{Mg}_{0.2}\text{O}_3$  at higher temperatures for a long time needs to be avoided in the fabrication process.

The lattice constants of  $\text{La}_{0.9}\text{Sr}_{0.1}\text{Ga}_{0.8}\text{Mg}_{0.2}\text{O}_3$  samples treated at different conditions are shown in Table 2. The impurity peaks were not included in the lattice parameter refinements. The cell volume after TG-DTA analyses up to 1200 °C in wet air and 9% $\text{H}_2$  is almost equal to that of the original  $\text{La}_{0.9}\text{Sr}_{0.1}\text{Ga}_{0.8}\text{Mg}_{0.2}\text{O}_3$  powder because the heating time at high temperature is not enough to cause obvious phase separation. However, the cell volume of the sample after heating at 1000 °C for approximately 130 h is 238.39 Å<sup>3</sup>, higher than the value 237.74 Å<sup>3</sup> for the original  $\text{La}_{0.9}\text{Sr}_{0.1}\text{Ga}_{0.8}\text{Mg}_{0.2}\text{O}_3$  obtained at 1500 °C, which is attributed to the segregation of  $\text{La}_4\text{SrO}_7$  and  $\text{SrLaGaO}_4$  from the parent phase.

After being fabricated at higher temperatures, a fuel cell using  $\text{La}_{0.9}\text{Sr}_{0.1}\text{Ga}_{0.8}\text{Mg}_{0.2}\text{O}_3$  as the electrolyte would usually operate at an intermediate temperature, e.g. 750 °C. Thus, the material was heated and weighed at 750 °C in dry and wet  $\text{H}_2$  for a long time to determine its stability at intermediate temperatures. The results are listed in Table 3. The weight only decreases 0.06% after heating in dry hydrogen at 750 °C for 84 h. Compared to 4.24% in dry  $\text{H}_2$  at 1000 °C in Table 1, it is insignificant. However, the weight increases 0.15% after heating at 750 °C in wet hydrogen for 48 h. Fig. 6(b) shows the XRD patterns of the sample after conventional weight analyses at 750 °C. The pattern is almost identical to the pattern obtained before the heat treatment [Fig. 6(a)]. The lattice parameters of the two samples are therefore unchanged within the standard deviation, as shown in Table 2. The phase segregation is insignificant at 750 °C. It is apparent that the

material is relatively stable at this temperature. However, for a practical fuel cell that should run for several years, the long-term stability of  $\text{La}_{0.9}\text{Sr}_{0.1}\text{Ga}_{0.8}\text{Mg}_{0.2}\text{O}_3$  would need to be further investigated.

### 3.4 Defect chemistry modelling

For the sake of generality we will consider a perovskite defect model, which can allow for variations in oxygen stoichiometry in LSGM, but also the possible presence of protonic defects. The argument for including protons is as follows: a systematic difference in weight was noticed between dry and wet atmosphere (see Fig. 7). Although LSGM has a transport number close to unity for oxygen ion,<sup>1</sup> and attempts to measure protonic conductivity in LSGM have so far failed,<sup>19</sup> non-conducting protons could still be present in LSGM.

The main volume fraction of the samples after heating to 1000 °C for 12–14 h is still a La–Ga-based perovskite phase, which has to account for some of the weight change observed, apart from the loss of  $\text{Ga}_2\text{O}_3$  by vaporisation under highly reducing conditions. The 10 weight measurements at 1000 °C, discussed in section 3.3, are, in principle, sufficient to determine the three equilibrium constants, describing the system, see eqn. (9–11) below. However, the weight data were not obtained *in situ*, nor by quenching. The extraction of three equilibrium constants from weight data obtained from equilibration at series of different  $P_{\text{O}_2}$  and  $P_{\text{H}_2\text{O}}$  pressures is demonstrated below.

A general defect description for a non-stoichiometric, proton containing perovskite, also including cation vacancies in  $\text{A}_q\text{B}_{1-p}\text{Mf}_p\text{O}_{3 \pm \epsilon}$ , was recently given by Poulsen.<sup>15</sup> In the present case we restrict our model to describe a perovskite with a ratio  $A/B = 1$ , and with no cation vacancies. The mathematical procedure of Bonanos and Poulsen,<sup>16</sup> originally developed for quantitative defect chemistry calculations on  $\text{SrCe}_{1-p}\text{Y}_p\text{O}_{3-p/2 \pm \delta}$ , can directly be transferred to the  $\text{La}_{1-x}\text{Sr}_x\text{Ga}_{1-y}\text{Mg}_y\text{O}_{3 \pm \epsilon}$  case, since the dopants in both systems have a valence one lower than the respective host lattice ions. It is found that the mathematics are identical when setting  $p = y + x$ . The following quartic equation in concentration arises:

$$\beta \cdot u^4 + (6-p) \cdot u^3 + (\beta - \alpha) \cdot u^2 - p \cdot u - \alpha = 0 \quad (4)$$

where  $u$  substitutes for:

$$u = \{[\text{Vo}]/(3 - [\text{Vo}])\}^{1/2} \quad (5)$$

$$\alpha = K_e^{1/2} \cdot P_{\text{O}_2}^{-1/4} \quad (6)$$

$$\beta = K_H^{1/2} \cdot P_{\text{H}_2\text{O}}^{1/2} + K_h^{1/2} \cdot P_{\text{O}_2}^{1/4} \quad (7)$$

where  $K_H$  and  $K_e$  are the  $K$ -values for eqn. (1a) and (3a) of ref. 16, respectively.

For a known atmosphere,  $P_{\text{H}_2\text{O}}$  and  $P_{\text{O}_2}$ , total dopant level,  $p$ , and assumed values of the three equilibrium constants, eqn. (4) can be solved by Newton–Raphson iteration using the analytical derivative of eqn. (4) and  $u = 0.5$  as a starting value. The four defect concentrations of interest are then determined as:

**Table 2** Lattice constants of  $\text{La}_{0.9}\text{Sr}_{0.1}\text{Ga}_{0.8}\text{Mg}_{0.2}\text{O}_{3-x}$  samples treated under different conditions

Lattice constants	Sample				
	Obtained at 1500 °C	After TG-DTA analysis in wet air	After TG-DTA analysis in 9% $\text{H}_2$ –91% $\text{N}_2$	After weight analysis at 1000 °C	After weight analysis at 750 °C
$a/\text{Å}$	5.5340(14)	5.5357(12)	5.5324(08)	5.5408(27)	5.5296(23)
$b/\text{Å}$	5.5074(22)	5.5069(18)	5.5070(11)	5.5150(28)	5.4991(47)
$c/\text{Å}$	7.8003(31)	7.7992(29)	7.8017(21)	7.8013(57)	7.8099(50)
Cell volume/Å <sup>3</sup>	237.74(19)	237.76(16)	237.69(12)	238.39(34)	237.48(20)

**Table 3** Weight and colour change of  $\text{La}_{0.9}\text{Sr}_{0.1}\text{Ga}_{0.8}\text{Mg}_{0.2}\text{O}_{3-x}$  in different atmospheres at 750 °C

Atmosphere	Dry air, 12 h	Dry pure H <sub>2</sub> , 84 h	Wet H <sub>2</sub> (0.6 vol% H <sub>2</sub> O), 48 h
Weight/g	0.6764	0.6760	0.6774
$(W_g - W_{\text{air}})/W_{\text{air}} \times 100$ (%) <sup>a</sup>	0	-0.06	+0.15
Colour	brown	grey	grey

<sup>a</sup> $W_g$  is the weight of sample in different atmospheres.  $W_{\text{air}}$  is the weight of sample in dry air.

$$[\text{Vo}] = 3 \cdot u^2 / (u^2 + 1) \quad (4)$$

$$[\text{H}_i] = K_{\text{H}}^{1/2} \cdot P_{\text{H}_2\text{O}}^{1/2} \cdot u \quad (9)$$

$$[\text{h}] = K_{\text{h}}^{1/2} \cdot P_{\text{O}_2}^{1/4} \cdot u \quad (10)$$

$$[\text{e}'] = K_{\text{e}}^{1/2} \cdot P_{\text{O}_2}^{-1/4} \cdot u^{-1} \quad (11)$$

The theoretical (calculated) relative weight change of one formula unit of perovskite, calculated in atomic mass units (AMU) is given by:

$$\Delta m_{\text{calc}} = \{16 \cdot (3 - [\text{Vo}]) + 1 \cdot [\text{H}_i]\}_{P_{\text{H}_2\text{O}}, P_{\text{O}_2}} - \{16 \cdot (3 - [\text{Vo}]) + 1 \cdot [\text{H}_i]\}_{\text{ref}} \quad (12)$$

where the calculated weight at  $P_{\text{H}_2\text{O}} = 8.4 \times 10^{-4}$  atm (dry) or  $6 \times 10^{-3}$  atm (wet), and  $P_{\text{O}_2} = 0.21$  atm are chosen as reference states. By using the non-linear least squares regression technique, values of the three equilibrium constants which minimise the residual  $\Sigma(\Delta m_{\text{calc}} - \Delta m_{\text{obs}})^2$  can be searched for. Fig. 7 shows two theoretically generated weight curves for the dry and wet series, along with the experimentally observed relative weights. The best fit was obtained with the following equilibrium constants at 1000 °C:  $K_{\text{H}} = 1940 \text{ atm}^{-1}$ ,  $K_{\text{h}} = 11.0 \text{ atm}^{-1/2}$ , and  $K_{\text{e}} = 4.5 \text{ atm}^{1/2}$ . The estimated uncertainties for these parameters are about  $\pm 25\%$ . The theoretically predicted weight curves, based on these values, apparently match the measurements quite well, apart from the measurement in 1 atm of oxygen, where the relatively large weight gain could not be accounted for.

However, other physical properties predicted from the three  $K$ -values are *not* physically acceptable. The predicted oxygen stoichiometries,  $\text{O}/(\text{Ga} + \text{Mg})$ , are 2.73 and 2.30 for the two most reducing measurements in wet and dry atmosphere, respectively. The latter oxygen content is far below what a perovskite requires. Also, the proton uptake amounts to 0.7 and 0.98 mol H per formula unit, respectively, which is far above any realistic level. It is apparent from the defect modelling that structural and other supplementary data are required along with the gravimetric data. Interpretation of the weight data alone would have led us to the false conclusion that doped  $\text{LaGaO}_3$  becomes highly sub-stoichiometric and contains massive amounts of protons, even in moderately wet (0.6% H<sub>2</sub>O) atmospheres. One possible reason for the higher weight in humid atmospheres than in dry ones could be the formation of oxyhydroxides or hydroxides, such as  $\text{La}(\text{OH})_3$  found by Yamaji *et al.*,<sup>14</sup> although these remained undetected in our samples. As described above, the modelling resulted in  $K$ -values predicting non-physical properties as well as unrealistic oxygen stoichiometries. The basic assumption for this modelling that the material is single phase does not hold.

## 4 Conclusions

The oxygen-ion conductor  $\text{La}_{0.9}\text{Sr}_{0.1}\text{Ga}_{0.8}\text{Mg}_{0.2}\text{O}_3$  has been prepared by a sol-gel process. The weight of the materials is related to oxygen and water vapour partial pressure. At 1000 °C, the  $\text{La}_{0.9}\text{Sr}_{0.1}\text{Ga}_{0.8}\text{Mg}_{0.2}\text{O}_3$  phase is unstable. The

impurity phases  $\text{La}_4\text{SrO}_7$  and  $\text{SrLaGaO}_4$  separate from the parent phase, which may destroy the structure of the doped oxygen-ion conductor. Therefore, heating the materials at high temperature for a long time should be avoided. After heating the material at 750 °C in H<sub>2</sub> atmosphere for a total of 132 h, no phase change was detected, indicating that  $\text{La}_{0.9}\text{Sr}_{0.1}\text{Ga}_{0.8}\text{Mg}_{0.2}\text{O}_3$  is relatively stable at intermediate temperatures. The question of the long term stability of  $\text{La}_{0.9}\text{Sr}_{0.1}\text{Ga}_{0.8}\text{Mg}_{0.2}\text{O}_3$  at intermediate temperatures, however, still deserves further investigation before LSGM can be used as an electrolyte in fuel cells.

A general procedure for determining equilibrium constants for perovskites equilibrated in different water vapour and oxygen partial pressures is given. The present LSGM weight data could be modelled, but other non-physical properties follow from the equilibrium constants obtained. The modelling thereby supports the findings from X-ray diffraction that LSGM kept for long periods of time at 1000 °C is not single phase.

## Acknowledgements

The authors are grateful to Dr Nikolaos Bonanos and Dorte Lybye of the Materials Research Department, Risø National Laboratory, for advice and a critical reading of the manuscript. Thanks to Knud Jensen, Torben Strauss and Palle Jensen for data collection. One of the authors (S. Tao) would like to thank the Danida Fellowship Centre for financially supporting his work at Risø.

## References

- 1 T. Ishihara, H. Matsuda and Y. Takita, *J. Am. Chem. Soc.*, 1994, **116**, 3801.
- 2 T. Ishihara, H. Matsuda and Y. Takita, *Solid State Ionics*, 1995, **79**, 147.
- 3 M. Feng, J. B. Goodenough, K. Q. Huang and C. Milliken, *J. Power Sources*, 1996, **63**, 47.
- 4 K. Q. Huang, M. Feng and J. B. Goodenough, *J. Electrochem. Soc.*, 1997, **144**, 3620.
- 5 P. N. Huang and A. Petric, *J. Electrochem. Soc.*, 1996, **143**, 1644.
- 6 T. Yamada, Y. Hiei, T. Akbay, T. Ishihara and Y. Takita, *Solid State Ionics*, 1998, **113–115**, 253.
- 7 T. Ishihara, T. Akbay, H. Furutani and Y. Takita, *Solid State Ionics*, 1998, **113–115**, 585.
- 8 J. Drennan, V. Zelizko, D. Hay, F. T. Ciacchi, S. Rajendran and S. P. S. Badwal, *J. Mater. Chem.*, 1997, **7**, 79.
- 9 J. Wolfenstine, P. Huang and A. Petric, *Solid State Ionics*, 1999, **118**, 257.
- 10 S. W. Tao, Z. L. Zhan, P. Wang and G. Y. Meng, *Solid State Ionics*, 1999, **116**, 29.
- 11 F. L. Chen, O. T. Sørensen, G. Y. Meng and D. K. Peng, *J. Mater. Chem.*, 1997, **7**, 481.
- 12 N. Bonanos, K. S. Knight and B. Ellis, *Solid State Ionics*, 1995, **79**, 161.
- 13 E. Djurado and M. Labeau, *J. Eur. Ceram. Soc.*, 1998, **18**, 1397.
- 14 K. Yamaji, T. Horita, M. Ishikawa, N. Sakai and H. Yokokawa, *Solid State Ionics*, 1999, **121**, 217.
- 15 F. W. Poulsen, *J. Solid State Chem.*, 1999, **143**, 115.
- 16 N. Bonanos and F. W. Poulsen, *J. Mater. Chem.*, 1999, **9**, 431.
- 17 S. W. Tao, Q. Y. Wu, Z. L. Zhan and G. Y. Meng, *Solid State Ionics*, 1999, **124**, 53.
- 18 D. Lybye, F. W. Poulsen and M. Mogensen, *Solid State Ionics*, 2000, **128**, 91.
- 19 T. Norby, personal communication, 1999.